frontiers | Frontiers in Earth Science

TYPE Original Research
PUBLISHED 16 July 2025
DOI 10.3389/feart.2025.1551085

OPEN ACCESS

EDITED BY
Yanbin Li,
Ocean University of China, China

REVIEWED BY
William Gibson Parker,
National Park Service, United States
Xiangdong Wang,
China University of Geosciences
Wuhan, China

*CORRESPONDENCE
Lucas Silveira Antonietto,
antoniettols@gmail.com

RECEIVED 24 December 2024
ACCEPTED 26 May 2025
PUBLISHED 16 July 2025

CITATION
Antonietto LS, Hamid I, Holgado B, Rocha AL, Ferreira MA, Saraiva AÁF, Lacerda LDd and Silva RCd (2025) Reconstructing paleotrophic relationships on the Brazilian Romualdo Formation (Lower Cretaceous) through mercury analysis in fossils.
Front. Earth Sci. 13:1551085.
doi: 10.3389/feart.2025.1551085

Reconstructing paleotrophic relationships on the Brazilian Romualdo Formation (Lower Cretaceous) through mercury analysis in fossils

Lucas Silveira Antonietto[1]*, Igor Hamid[2], Borja Holgado[1,3], Antonio Leite Rocha[4], Maria Andréia Ferreira[2], Antônio Álamo Feitosa Saraiva[4], Luiz Drude de Lacerda[2] and Rafael Costa da Silva[5]

[1]Museu de Paleontologia Plácido Cidade Nuvens, Regional University of Cariri, Santana do Cariri, Brazil, [2]Instituto de Ciências do Mar, Federal University of Ceará, Fortaleza, Brazil, [3]Institut Català de Paleontologia Miquel Crusafont, Universitat Autònoma de Barcelona, Barcelona, Spain, [4]Laboratório de Paleontologia da URCA, Centro de Ciências Biológicas e da Saúde, Regional University of Cariri, Crato, Brazil, [5]Earth Sciences Museum, Geological Survey of Brazil, Rio de Janeiro, Brazil

Mercury (Hg) biomagnification values tend to reflect relationships between species in the trophic web, where larger values indicate higher positions in the web. Herein, we present a pioneering attempt to reconstruct the paleotrophic linkages during the onset of the Romualdo Formation in the Araripe Basin (northeastern Brazil) based on analyses of the Hg concentrations ([Hg]) in fossil specimens recorded in this lithological unit. To understand these relationships, several vertebrate taxa were analyzed through cold vapor generation atomic absorption spectrometry (CV-AAS) to quantify [Hg] in both fossils ($[Hg]_{Fossil}$) and their surrounding concretions ($[Hg]_{Rock}$). The observed ratios ($log[Hg]_{Sample}$) indicate greater biomagnification with changes in the feeding habits and sizes of the evaluated vertebrate taxa; the lowest values were observed in the small actinopterygian fish genera *Rhacolepis* and *Tharrhias* while the peak values were noted in large predators like *Cladocyclus* and *Calamopleurus* (apex species of the trophic pyramid). The feeding habits of *Vinctifer* were also reviewed, and the genus was reinterpreted from a filter feeder to a mesopredator; *Neoproscinetes* and an unidentified batoid ray (*Chondrichthyes*) were two durophagous bottom-feeding taxa that showed values compatible with their predicted feeding habits. Low values of the $log[Hg]_{Sample}$ ratios were observed in the ornithocheiraean pterosaurs (Reptilia), suggesting these were mesopredators specializing in smaller fish species, while Thalassodrominae presented intermediate-to-high $log[Hg]_{Sample}$ values, indicating their unique trophic role as terrestrial opportunistic generalists, ranging from predators to scavengers.

KEYWORDS

Araripe Basin, geochemistry, mercury cycle, paleoecology, Vertebrata

1 Introduction

In this work, we use mercury concentration ([Hg]) analysis to reconstruct the trophic relationships among the taxa of the exceptionally preserved and highly diverse fossil assemblages of the Lower Cretaceous (Aptian–Albian) Romualdo Formation in the Araripe Basin of northeastern Brazil. The assemblage evaluated herein comprises several pristine vertebrate specimens, including the Chondrichthyes (cartilaginous fish) and Actinopterygii (ray-finned fish) of the Holostei (amiids) and Teleostei (teleosts) groups as well as Tetrapodomorpha of the Pterosauria (pterosaurs) group. Despite the relevance of the proposed results on pterosaurs (which are mostly in agreement with previous morphology-based analyses of trophic relations between the pterosaur and fish species), these data are considered preliminary owing to small sampling size.

Mercury (Hg) is a chemical element that is widely distributed throughout the biosphere, its dispersion linked to atmospheric emissions by active volcanic chains and forest fires (Beckers and Rinklebe, 2017). Once released into the atmosphere, Hg circulates between the atmospheric, terrestrial, and oceanic reservoirs in its organic and inorganic forms (Pyle and Mather, 2003; Sun et al., 2019). During the atmospheric stage of its cycle, the elementary form of Hg (Hg^0) undergoes oxidation to generate the more reactive, water-soluble Hg^{2+} (Figure 1); this form is incorporated into aquatic ecosystems to form stable organic complexes (Grasby et al., 2019) that either undergo adsorption into clay minerals (Sial et al., 2013; Font et al., 2016) or precipitate into sulfides in bottom sediments (Gamboa Ruiz and Tomiyasu, 2015; Beckers and Rinklebe, 2017). In sediments, Hg can undergo methylation mediated by sulfate-reducing bacteria to generate methylmercury (MeHg) – a bioavailable form of Hg (Luo et al., 2020). Several microorganisms (sulfate-reducing and nitrifying bacteria as well as methanogenic archaea) play significant roles in the production of MeHg in aquatic environments (Wang Y. et al., 2020; Starr et al., 2022; Wang J. et al., 2022).

Mercury enters biological systems via two principal mechanisms: bioaccumulation (increase in [Hg] in organisms with age or size) and biomagnification (increase within food webs according to the trophic statuses of the species) (Benoit et al., 2003; Campbell et al., 2003). Over the course of geological time, Hg accumulations have been occasionally preserved, especially in fossil records, owing to the interactions with minerals commonly found in mineralized tissues, such as apatite (including hydroxyapatite, carboxyapatite and post-diagenetic fluorapatite), calcite, and aragonite (Cardia et al., 2018; Kim et al., 2018; Cervini-Silva et al., 2021). Bone apatite is particularly prone to Hg bioaccumulation/biomagnification, and its incorporation into post-mortem remains by diagenesis is diminished even in Hg-rich strata (Emslie et al., 2019). Calcium (Ca) atoms in skeleton-forming minerals are commonly displaced by Hg—a process facilitated by similarities in the electrical charges and ionic radii between Ca^{2+} and Hg^{2+} (Kępa et al., 2012; Ávila et al., 2014). The reaction with carboxyapatite is summarized by the following equation (Cervini-Silva et al., 2021):

$$Ca_{10}(PO_4)_4(CO_3)_3(OH) + 5Hg^{2+} \rightarrow Hg_3PO_4\left[(Hg_2)_3(PO_4)_2\right]$$

An examination of Hg distribution across geological time has revealed a correlation between its anomalous deposition and activation of large igneous provinces, major paleoclimatic shifts and mass extinction events (Rampino et al., 2024; Zhou et al., 2024). Anomalous Hg levels have been documented in the Late Ordovician (Bond and Grasby, 2020; Sial et al., 2024), Late Devonian (Racki et al., 2018), Permian–Triassic (Sanei et al., 2012; Sial et al., 2021), end-Triassic (Thibodeau et al., 2016), and Cretaceous–Paleogene (Font et al., 2016; Sial et al., 2016) extinctions. The applicability of Hg in reconstructing the paleoecological aspects of fossil records is well known: Late Cretaceous baurusuchid crocodiles have been distinguished into several ontogenetic levels based on [Hg] from eggs, bones, teeth, and osteoderms (Cardia et al., 2018). Meyer et al. (2019) also documented a correlation between elevated Hg bioaccumulation in mollusks and the activation of Deccan volcanism. Murray et al. (2015) evaluated [Hg] in living and subfossil (Holocene) codfish and found the influences of sea-level variations during that period.

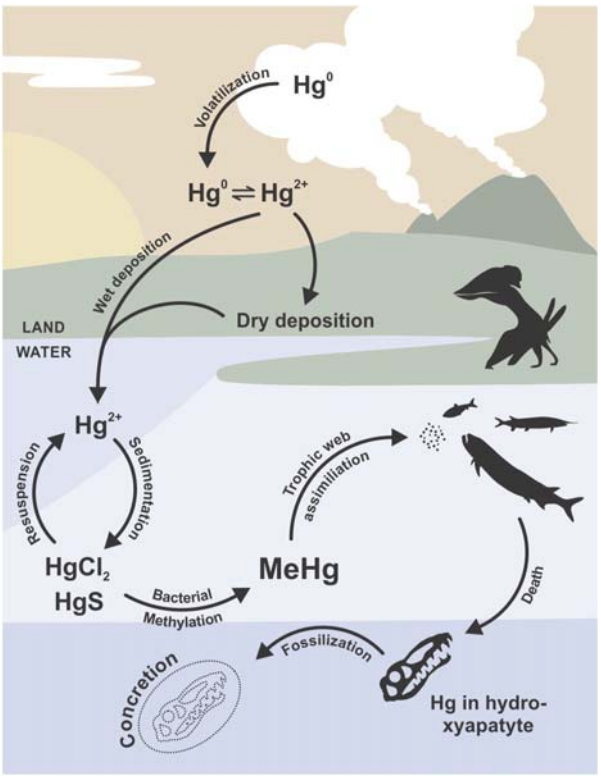

FIGURE 1
Mercury (Hg) cycle until preservation in the apatite of fossilized bones (modified from Cardia et al. (2018) and Grasby et al. (2019)).

2 Geological setting

Assessments of [Hg] in fossil mineralized tissues are heavily dependent on exceptional preservation, such as observed in specimens of the konservat-laggerstätte of the Romualdo Formation of Brazil. This unit is the result of a regional-scale, late Aptian - early Albian transgression (Araripe et al., 2022) during the opening of the South Atlantic Ocean that reached many interior regions of northeastern Brazil, including the Araripe Basin (Custódio et al.,

2017). Such conditions favored the deposition throughout the unit of several stratigraphic horizons abundant in carbonate concretions; some of these have yielded finely preserved skin, muscle, vascular systems and 3D organs of several vertebrate species (Kellner and Campos, 1994; Kellner, 1996a, Kellner, 1996b; Martill, 1988; Maldanis et al., 2016). Stomach contents are also frequently available; the diets of these specimens (Maisey, 1994) and their oral morphologies (Lopes and Barreto, 2021) have been utilized previously to establish trophic relations in the Romualdo assemblage.

Romualdo concretions not only preserve fossils pristinely but also maintain their chemical compositions over time. Isotope ($\delta^{13}C$, $\delta^{18}O$, and $^{87}Sr/^{86}Sr$) (Heimhofer et al., 2017), X-ray diffraction, and spectroscopy (Lima et al., 2007; Freire et al., 2014; Sousa Filho et al., 2016; Barros et al., 2019) analyses have indicated low interference from diagenetic processes, maturation under ambient temperatures, and distinct mineralogical compositions between the preserved fossils acting as nucleators of the concretion and their surrounding matrices. Such samples are also abundant, and numerous specimens are available in scientific collections of several Brazilian institutions, including: Museu de Paleontologia Plácido Cidade Nuvens (MPPCN) in the City of Santana do Cariri, Laboratório de Paleontologia da URCA (LPU) in Crato (Saraiva et al., 2021), Museu de Ciências Naturais e História de Barra do Jardim (MCNHBJ) in Jardim (Coutinho et al., 2021), and Earth Sciences Museum in (MCTer) Rio de Janeiro. Therefore, Hg assessments of samples from Romualdo concretions and their fossil contents can be powerful tools for reconstructing trophic webs of both recent and fossilized assemblages.

3 Materials and methods

3.1 Constraints on acquiring vertebrate specimens for destructive analyses

All Romualdo specimens used in the present work were sourced from the scientific collections of the MPPCN, LPU, MCNHBJ and MCTer (Figure 2). Seven fish species were selected based on their availability and presumed ecological roles (Wilby and Martill, 1992; Maisey, 1994; Silva Santos, 1995; Brito, 1997; Lopes and Barreto, 2021): *Rhacolepis buccalis* (n = 5), *Vinctifer comptoni* (n = 5), *Cladocyclus gardneri* (n = 3), *Calamopleurus cylindricus* (n = 6), *Tharrhias araripis* (n = 2), *Neoproscinetes penalvai* (n = 2), and an unidentified species of Batoidea (n = 2). Additional specimens of pterosaurs identified as Ornithocheirae (n = 3), Thalassodrominae (n = 1) and unidentified ornithocheiroid specimens (n = 2) were included in this study.

Considering the [Hg] analysis is destructive in nature, it is important to emphasize that none of the fossil specimens deployed in the present study were type materials. To avoid loss of taxonomically relevant specimens, we relied on species with large fossil recovery in the Araripe. For the pterosaurs, only those body parts that are not particularly rich in apomorphies (such as pterosaur phalanges, limb bones, and cranial fragments) were used – which impacted the numbers of samples of some taxa as well as their depth of taxonomic identification. The same was true for some of the batoid rays, for which none of the recovered specimens were as complete as the type materials of currently known species in the Romualdo.

3.2 Mercury quantification and [Hg] calculation

All specimens were processed at the LPU, where samples of approximately 7 cm^3 were sawed off with a Makita M0400B circular saw. The resulting slabs were sent as separate samples to the Marine Science Institute (LABOMAR) of the Federal University of Ceará, Fortaleza, Brazil, for [Hg] analysis. Detailed summaries of the methods used in lab preparations and [Hg] analyses are available in Benigno et al. (2021) and Hamid et al. (2024), which are provided herewith as supplementary data. Measurements were performed on both fossils and the carbonate matrices of their surrounding concretions; we used [Hg] in the concretions ($[Hg]_{Rock}$) as the normalizer for environmental effects over fossils ($[Hg]_{Fossil}$), and applied the following ratio to quantify [Hg] bioaccumulation in the sample:

$$[Hg]_{Sample} = [Hg]_{Fossil}/[Hg]_{Rock}$$

The ratio was normalized, and a generalized linear model was applied to determine the different trophic levels based on [Hg]. In this case, the logarithm of the concentration (y = log[Hg]) was used as the response variable to enable the identification of outliers (Trevizani et al., 2021). Additional statistical analyses were performed using RStudio© software (v. 4.3.3).

4 Results and discussion

4.1 Hg biomagnification in recent estuaries versus the paleoenvironment of the Romualdo formation

Chiang et al. (2021) provided a complete model for biomagnification values in the evaluated taxa of the Romualdo Formation; this work relied on the modern trophic webs of Patagonia and Antarctica, where different mammals (cetaceans and pinnipeds), birds and fish represent the various predatory roles of pterosaurs and fish from Romualdo paleoenvironments. Similar scenarios (with smaller-scale trophic chains) were observed by Trevizani et al. (2021), Muto et al. (2014), Hosseini et al. (2013), and Qu et al. (2022) in the tropical estuaries of southeastern Brazil, Iran, and China. Compared to these areas, [Hg] in the Romualdo exhibits an additional tendency toward increased biomagnification (Table 1) from micropredators to mesopredators to durophagous predators, reaching the highest values in the apex species *C. cylindricus*.

We observed that despite their low $log[Hg]_{Sample}$ values in comparison to other evaluated taxa, some specimens of *R. buccalis* and *V. comptoni* show the highest $[Hg]_{Fossil}$ and $[Hg]_{Rock}$ values among the analyzed specimens. Chiang et al. (2021), Trevizani et al. (2021), and Qu et al. (2022) all emphasize proximity to Hg sources (especially those of anthropic origin) as the main factor for Hg bioaccumulation. The lack of the anthropic factor led us to consider other reasons for these accumulated concentrations, such as the

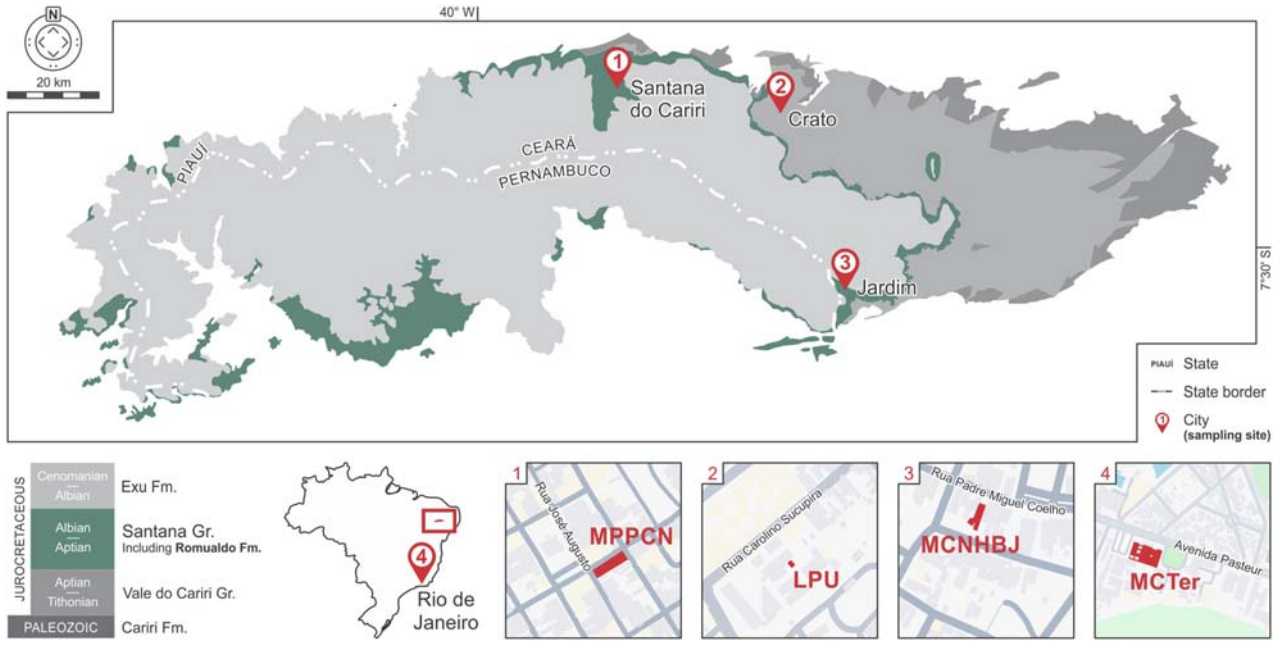

FIGURE 2
Map of the Araripe Basin in northeastern Brazil showing the geographical distribution of the Santana Group (including the Romualdo Formation) (modified from Rosa et al. (2023)). The museums and laboratories whose curated sample collections were used in this work are also highlighted.

role of volcanos as sources (Pyle and Mather, 2003) and rivers as transporters of Hg into larger bodies of water (Chiang et al., 2021).

The concretion-rich shales of the Romualdo were deposited in large water bodies, ranging from lagoons to an epicontinental sea, that varied widely in terms of the salinity (Fürsich et al., 2019), owing to substantial contributions of meteoric waters being carried into the basin by riverine systems (Bom et al., 2023). Both *R. buccalis* and *V. comptoni* featured among the smallest fish species of the Romualdo and may have sought refuge near the shores (even if only through part of their life cycle). Living in such benthic conditions, where total Hg and MeHg availabilities are considerably higher (Chételat et al., 2015), would make them more prone to Hg accumulation than larger, more pelagic species. One of the probable sources to the Romualdo could be the Aptian Southern Kerguelen Plateau volcanic event (Hamid et al., 2024); there is also strong evidence of secondary sources in wildfires that may have heavily affected the paleobiota of the Romualdo (Lima et al., 2019).

4.2 Trophic relationships between fish species

Absolute and average $\log[Hg]_{Sample}$ results of analyzed species are summarized in Figure 3. Lower trophic levels of the Romualdo taxa (represented by smaller species with villiform dentition) (Lopes and Barreto, 2021) showed lesser $\log[Hg]_{Sample}$ values: *R. buccalis* (−1.14 to −0.37); *T. araripis* (−0.06 and −0.07); *V. comptoni* (−0.50 to 0.30). Considering these $\log[Hg]_{Sample}$ values and historical records of stomach contents of *T. araripis* and *R. buccalis*, we hypothesized these organisms probably fed on decapod crustaceans and smaller fish (Maisey and Carvalho, 1995). The presence of gill rakers and microbranchiospines in *R. buccalis* (Ribeiro et al., 2020) suggest it could be ecologically equivalent to the milkfish (*Chanos*), a benthopelagic species with similar [Hg] levels and diet (Hosseini et al., 2013).

The position of *V. comptoni* in the Romualdo food web, based on the stomach content analyses of some specimens, has been previously inferred as that of a mesopredator feeding on smaller fish (Wilby and Martill, 1992; Brito, 1997; Coutinho et al., 2021) - although there are no published images detailing these findings. Maisey (1994) found no small fish fragments during stomach content analysis of *V. comptoni*, instead linking its reduced dentition and well-developed gill apparatus to morphologies observed in recent filter-feeding taxa, such as paddlefishes (genus *Polyodon*). Observed average $\log[Hg]_{Sample}$ values, however, indicate piscivore feeding habits, probably involving consumption of fish taxa like *T. araripis* and *R. buccalis* or even *Santanichthys diasii* (Silva Santos, 1995). Ratios also show large variability per specimen than other evaluated species, which is interpreted herein as a possible consequence of foraging variation tied to either geographical (Azad et al., 2019) and/or ontogenetic (Di Beneditto et al., 2013) factors.

$\log[Hg]_{Sample}$ values increase with the trophic level (transition from villiform to molariform to conical dentition, accompanied by an increase in the overall size of the species), indicating shifts to higher levels of the trophic web (Figure 4). Molariform mid-tier-level species evaluated in the present work include a species of ray listed as Batoidea indet. ($\log[Hg]_{Sample}$: −0.02 to 0.03) and *N. penalvai* ($\log[Hg]_{Sample}$: 0.03–0.06); these are interpreted as benthic durophagous taxa feeding on larger and opportunistic invertebrates, as described in Lopes and Barreto (2021) and Meunier et al. (2021). Based on dietary (Bornatowski et al., 2005) and [Hg] comparisons

TABLE 1 Mercury concentrations ([Hg]) in fossil vertebrate specimens ($[Hg]_{Fossil}$), surrounding concretions ($[Hg]_{Rock}$), bioaccumulations ($[Hg]_{Sample}$), and $[Hg]_{sample}$ averages of taxa from the Romualdo Formation in the Araripe Basin of northeastern Brazil.

Sample	Group	Taxon	Trophic functional group	$[Hg]_{Fossil}$	$[Hg]_{Rock}$	$[Hg]_{Sample}$	log ($[Hg]_{Sample}$)
MPPCN P 5357	Fish	*Rhacolepis buccalis*	Pelagic micropredator	34.65	482.67	0.07	−1.14
MPPCN P 5356				157.16	1,330.49	0.12	−0.93
MPPCN P 5358				105.25	304.62	0.35	−0.46
MPPCN P 5360				298.59	808.80	0.37	−0.43
MPPCN P 5359				41.25	95.68	0.43	−0.37
					Taxon average	0.267	−0.666
MCNHBJ 105	Flying reptile	Ornithocheiriformes	Pelagic mesopredator	3.85	17.92	0.21	−0.67
MCNHBJ 345				1.46	4.45	0.33	−0.48
MCT.R.1505	Flying reptile	Ornithocheiroidea indet.	Pelagic mesopredator	14.73	10.99	1.34	0.13
					Taxon average	0.271	−0.202
—	Fish	*Tharrhias araripis*	Pelagic micropredator	8.28	9.72	0.85	−0.06
—				17.72	20.11	0.88	−0.07
					Taxon average	0.867	−0.062
MPPCN P 5311	Fish	*Vinctifer comptoni*	Pelagic mesopredator	10.13	22.55	0.45	−0.35
MPPCN P 5314				6.73	12.29	0.55	−0.26
MPPCN P 5317				18.64	25.96	0.72	−0.14
MPPCN P 5313				111.29	125.68	0.89	−0.05
MPPCN P 5309				112.02	55.80	2.01	0.30
					Taxon average	0.922	−0.035
MCNHBJ 0353	Fish	Batoidea indet.	Benthic durophage	41.13	42.93	0.96	−0.02
MCNHBJ 0043				45.31	41.83	1.08	0.03
					Taxon average	1.021	0.009
MCNHBJ 0364	Fish	*Neoproscinetes penalvai*	Benthic durophage	31.22	28.89	1.08	0.03
MCNHBJ 134				34.29	29.59	1.16	0.06
					Taxon average	1.120	0.049
MPPCN P 2425	Fish	*Cladocyclus gardneri*	Pelagic predator	22.90	22.99	1.00	0.00
MPPCN P 2448				20.93	16.89	1.24	0.09
MPPCN P 2436				10.83	8.29	1.31	0.12
					Taxon average	1.181	0.072
MPPCN R 5038	Flying reptile	Thalassodrominae	Land predator	10.72	4.19	2.56	0.41
MPPCN R 1434	Flying reptile	Ornithocheiroidea indet.	Land predator?	10.91	4.14	2.64	0.42
MCT.LE.769	Flying reptile	Azhdarchoidea(?)	Land predator	50.47	10.55	4,78	0.68

(Continued on the following page)

TABLE 1 (*Continued*) Mercury concentrations ([Hg]) in fossil vertebrate specimens ($[Hg]_{Fossil}$), surrounding concretions ($[Hg]_{Rock}$), bioaccumulations ($[Hg]_{Sample}$), and $[Hg]_{sample}$ averages of taxa from the Romualdo Formation in the Araripe Basin of northeastern Brazil.

Sample	Group	Taxon	Trophic functional group	$[Hg]_{Fossil}$	$[Hg]_{Rock}$	$[Hg]_{Sample}$	log ($[Hg]_{Sample}$)
					Taxon average	2.598	0.522
CL-5	Fish	*Calamopleurus cylindricus*	Apex pelagic predator	5.16	10.34	0.50	−0.30
CL-7				6.44	8.81	0.73	−0.14
MPPCN P 5320				26.95	17.74	1.52	0.18
MPPCN P 5319				20.73	13.53	1.53	0.19
CL-1				20.00	11.90	1.68	0.23
MPPCN P 5354				202.16	9.59	21.08	1.32
					Taxon average	4.507	0.654

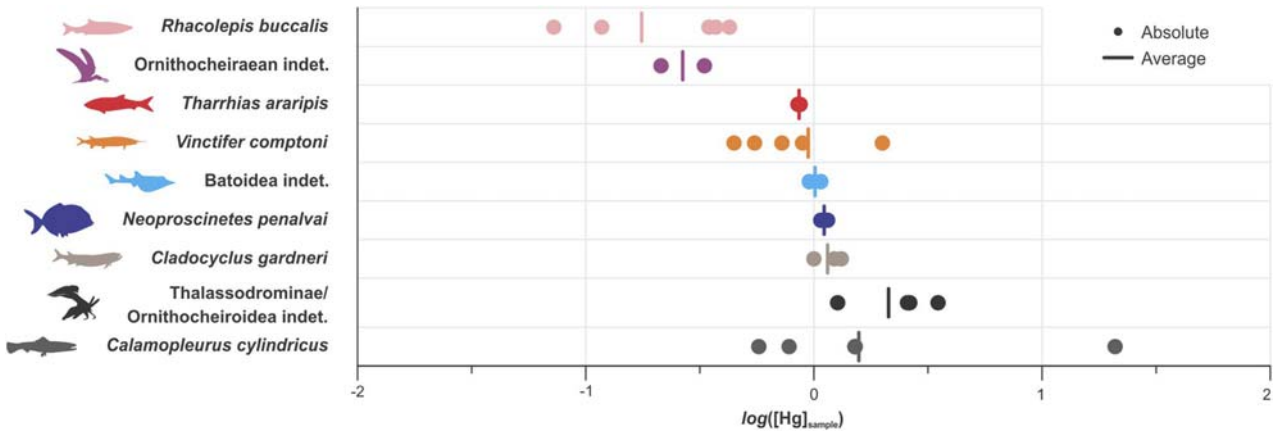

FIGURE 3
Average $log[Hg]_{sample}$ values in the fossil taxa of the Romualdo Formation analyzed in the present study.

(Muto et al., 2014), Batoidea indet. may be correlated with the modern guitarfish (*Zapteryx*) (Laurini, 2015; Lopes and Barreto, 2021). The modern analog for *N. penalvai* would be triggerfishes (*Ballistidae*) (Poyato-Ariza et al., 1998) - a mostly marine, eventually estuarine family, just as pycnodontids and other grazing durophages of Romualdo paleoenvironments (Nursall, 1996).

Individuals of *C. gardneri* and *C. cylindricus* displayed $log[Hg]_{Sample}$ values greater than 0.12, as expected for higher levels of the trophic web – occupied by the largest, conical teeth-bearing fish taxa of the Araripe. The highest $log[Hg]_{Sample}$ values (−0.30 to 1.32) were observed in specimens of *C. cylindricus*; these may have acted as apex predators in the aquatic environments of the Romualdo, able to feed on whatever fitted into their mouths (including cannibalizing other *C. cylindricus*) (Mulder, 2013). Despite being similar in size and tooth morphology, *C. gardneri* would occupy a pelagic ecological niche, feeding much closer to the surface than *C. cylindricus* (Lopes and Barreto, 2021). The observed differences in $log[Hg]_{Sample}$ not only support this ideation but also imply feeding habits of *C. cylindricus* could include the demersal realm. Therefore, ecological differences between these species would be similar to those observed in pelagic (*Thunnus albacares*) and demersal (*Thunnus obesus*) tuna, which also show ecologically-related disparities in Hg intake and biomagnification (Lacerda et al., 2017).

4.3 The role of pterosaurs as mesopredators and opportunists

Similar to *V. comptoni* and *C. cylindricus*, $[Hg]_{Sample}$ values in pterosaurs varied greatly; specimens attributed to the Ornithocheirae (ornithocheiraeans) showed very low $log[Hg]_{Sample}$ (−0.67 and 0.13) values slightly higher than the average observed for *R. buccalis*. Representatives of this clade have been commonly interpreted as highly capable piscivores based on dental morphology, geochemistry, and digestive tract content

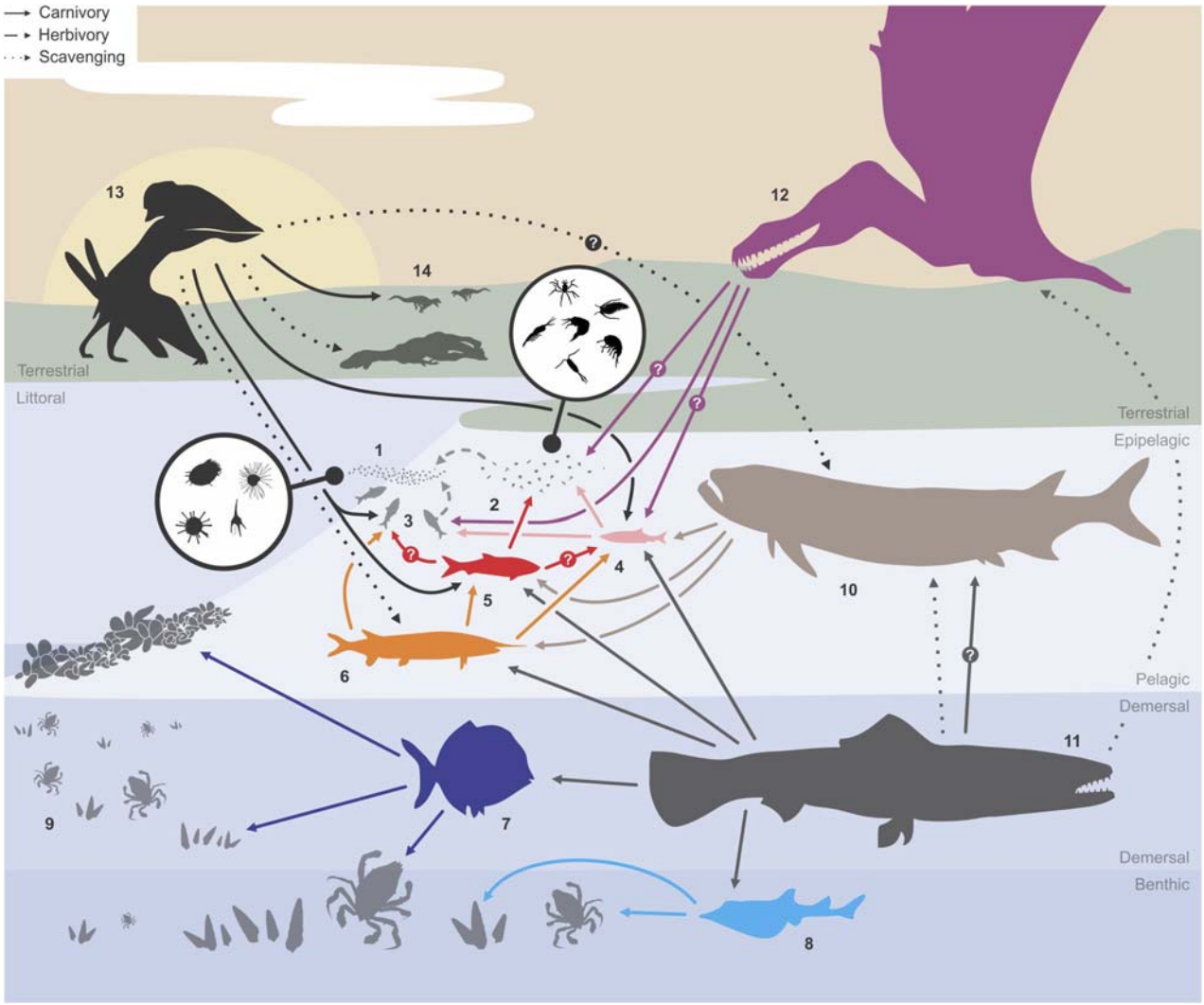

FIGURE 4
Summary of the Romualdo trophic web based on literature and the log[Hg]$_{sample}$ results of the present study for the following groups or taxa: (1) phytoplankton; (2) zooplankton; (3) *Santanichthys diasii*; (4) *Rhacolepis buccalis*; (5) *Tharrhias araripis*; (6) *Vinctifer comptoni*; (7) *Neoproscinetes penalvai*; (8) Batoidea indet.; (9) benthic invertebrates; (10) *Cladocyclus gardneri*; (11) *Calamopleurus cylindricus*; (12) Ornithocheiriformes; (13) Thalassodrominae; (14) other terrestrial Tetrapoda. Arrows indicate different feeding habits among the species of the paleotrophic web.

(Bestwick et al., 2018). However, present low bioaccumulation ratios suggest a foraging habit typical of mesopredators specializing in small epipelagic species of the Romualdo fish fauna, such as *R. buccalis* and *S. diasii* (Maisey, 1994; Lopes and Barreto, 2021). The presence of an air-sac system, inferred from their extremely extended skeletal pneumaticity, also indicates ornithocheiraeans could plunge after their prey (Holgado, 2020) like modern pelicans (Shoop and Tilson, 2022).

However, it is important to highlight the possible role of vital effect in our geochemical results, as sampling size of pterosaurs was quite small; nonetheless the observed value is identical to that for the undefined ornithocheiroid. Moreover, as in the case of *V. comptoni*, we cannot entirely discard the fact that the very low log[Hg]$_{Sample}$ values were obtained from a juvenile ornithocheiraean individual; further histological analyses of these lineages (Araújo et al., 2023) might help elucidate this observation. Chiang et al. (2021) suggested that the transfer of MeHg between trophic levels could be more efficient from prey to predators living in aquatic habitats than from these species to air-breathing vertebrates, even when they fed upon aquatic species.

Regarding the only specimen that was unambiguously attributed to the Thalassodrominae, the log[Hg]$_{Sample}$ value was significantly higher (0.42) than those of ornithocheiraeans. Thalassodromines were originally suggested to be piscivores with skim-feeding habits, but later studies proposed these creatures were terrestrially foraging opportunists because of the robust hind limbs observed in some thalassodromine specimens (Witton, 2013). The log[Hg]$_{Sample}$ results herein strengthen this opportunistic diet hypothesis, since higher ratios would be attainable only through a combination of varied predatory (small to mid-size prey) and scavenging behaviors, as suggested for all known thalassodromine taxa so far (Pêgas et al., 2021).

5 Conclusion

The findings of this study demonstrate fossils have the capacity to preserve biomagnified Hg content over geological time, through a combination of biological binding of Hg to apatite in vertebrate bones and preservation into diagenesis-resistant calcareous concretions. Concomitant measurements of [Hg] in fossils and their concretions is a reliable geochemical proxy for interpreting paleotrophic webs. Our inferences based on log[Hg]Sample values, quantified in species of the Aptian–Albian Romualdo Formation of Brazil, helped reconstruct the trophic relationships in this paleoenvironment.

Bioaccumulation ratios increased along the Romualdo food web based on taxon size and diet, as observed from small, filiform-toothed, small-prey specialist fish to the large, conical-toothed apex-predator that fed on the former (and many more taxa). In this scenario, values observed for *V. comptoni* favor an interpretation of its feeding habits as a mesopredatory species. Lesser $\log[Hg]_{Sample}$ values observed in some ornithocheiraean pterosaurs indicate they were also mesopredators, specializing in the smallest fish species of the assemblage. Molariform fish taxa occupied intermediate levels in the food web, typically consuming bottom-feeding invertebrates while being consumed in turn by *C. cylindricus*, the demersal apex predator/scavenger of Romualdo aquatic paleoenvironments - right above *C. gardnerii*, another powerful pelagic predator of the fauna. Meanwhile, thalassodromine pterosaurs presented intermediate-to-high $\log[Hg]_{Sample}$ values that place them in a more separate trophic role when compared to aquatic and water-dependent species: they were terrestrial generalists that not only preyed on small terrestrial taxa, but also could have engaged in scavenging remains of both terrestrial and aquatic taxa.

Data availability statement

The original contributions presented in this study are included in the article/Supplementary Material, and any further inquiries may be directed to the corresponding author.

Author contributions

LA: Conceptualization, Data curation, Funding acquisition, Investigation, Methodology, Project administration, Supervision, Validation, Visualization, Writing – original draft, Writing – review and editing. IH: Data curation, Formal analysis, Funding acquisition, Investigation, Methodology, Visualization, Writing – original draft, Writing – review and editing. BH: Investigation, Validation, Writing – original draft, Writing – review and editing. AR: Investigation, Resources, Writing – original draft. MF: Formal analysis, Investigation, Methodology, Writing – original draft. AS: Conceptualization, Data curation, Resources, Writing – original draft. LL: Funding acquisition, Methodology, Validation, Writing – original draft, Writing – review and editing. RS: Data curation, Formal analysis, Resources, Writing – review and editing.

Funding

The author(s) declare that financial support was received for the research and/or publication of this article. This study was supported by the Fundação Carlos Chagas Filho de Amparo à Pesquisa do Estado do Rio de Janeiro (FAPERJ: proc. no. E-26/210.294/2021 to RS), Fundação Cearense de Apoio ao Desenvolvimento Científico e Tecnológico (FUNCAP: proc. no. PV1-0187-00042.01.00/21 to LA; proc. no. PV1-0187-00054.01.00/21 to BH; proc. no. BP5-0197-00172.01.02/23 to AR), Brazilian Federal Agency for Support and Evaluation of Graduate Education (CAPES: proc. no. 88887.483498/2020-00 to IH Incorporação de gratificação no final do ano, mais 6%; proc. no. 407158/2022-7 to RS), and National Council for Scientific and Technological Development (CNPq) through the project "Instituto Nacional de Ciência e Tecnologia de Transferência de Materiais Continente-Oceano" (INCT-TMCOcean: proc. no. 405.765/2022-3 to LL).

Acknowledgments

The authors wish to acknowledge the staff at MCNHBJ (DLC Coutinho, JA Coutinho Júnior, and CC Coutinho) for their support providing fossil specimens for analyses in the present work.

Conflict of interest

The authors declare that the research was conducted in the absence of any commercial or financial relationships that could be construed as a potential conflict of interest.

Generative AI statement

The author(s) declare that no Generative AI was used in the creation of this manuscript.

Publisher's note

Supplementary material

The Supplementary Material for this article can be found online at: https://www.frontiersin.org/articles/10.3389/feart.2025.1551085/full#supplementary-material

References

Araripe, R. C., Pedrosa Lemos, F. A., do Prado, L. A. C., Tomé, M. E. T. R., Oliveira, D. H. D., Pereira, P. A., et al. (2022). Upper aptian–lower albian of the southern-central Araripe Basin, Brazil: microbiostratigraphic and paleoecological inferences. *J. South. Am. Earth. Sci.* 116, 103814. doi:10.1016/j.jsames.2022.103814

Araújo, E. V. de, Bantim, R. A. M., Holgado, B., Sayão, J. M., Weinschütz, L. C., and Kellner, A. (2023). Osteohistological characterization and ontogeny of *Caiuajara dobruskii* (Pterosauria, pterodactyloidea, tapejaridae). *Hist. Biol.* 36, 1204–1219. doi:10.1080/08912963.2023.2207193

Ávila, A., Mansilla, J., Bosch, P., and Pijoan, C. (2014). Cinnabar in mesoamerica: poisoning or mortuary ritual? *J. Archaeol. Sci.* 49, 48–56. doi:10.1016/j.jas.2014.04.024

Azad, A. M., Frantzen, S., Bank, M. S., Nilsen, B. M., Duinker, A., Madsen, L., et al. (2019). Effects of geography and species variation on selenium and mercury molar ratios in Northeast Atlantic marine fish communities. *Sci. Total Environ.* 652, 1482–1496. doi:10.1016/j.scitotenv.2018.10.405

Barros, O. A., Silva, J. H., Saraiva, G. D., Viana, B. C., Paschoal, A. R., Freire, P. T. C., et al. (2019). Physicochemical investigation of shrimp fossils from the Romualdo and ipubi formations (Araripe Basin). *Peer J.* 7, e6323. doi:10.7717/peerj.6323

Beckers, F., and Rinklebe, J. (2017). Cycling of mercury in the environment: sources, fate, and human health implications: a review. *Crit. Rev. Environ. Sci. Technol.* 47, 693–794. doi:10.1080/10643389.2017.1326277

Benigno, A. P. A., Saraiva, A. A. F., Sial, A. N., and Lacerda, L. D. (2021). Mercury chemostratigraphy as a proxy of volcanic-driven environmental changes in the Aptian-Albian transition, Araripe Basin, northeastern Brazil. *J. South. Am. Earth. Sci.* 107, 103020. doi:10.1016/j.jsames.2020.103020

Benoit, J. M., Gilmour, C. C., Heyes, A., Mason, R. P., and Miller, C. L. (2003). Geochemical and biological controls over methylmercury production and degradation in aquatic ecosystems. *ACS Symp. Ser.* 835, 262–297. doi:10.1021/bk-2003-0835.ch019

Bestwick, J., Unwin, D. M., Butler, R. J., Henderson, D. M., and Purnell, M. A. (2018). Pterosaur dietary hypotheses: a review of ideas and approaches. *Biol. Rev.* 93, 2021–2048. doi:10.1111/brv.12431

Bom, M. H. H., Kochhann, K. G. D., Heimhofer, U., Mota, M. A. L., Guerra, R. M., Simões, M. G., et al. (2023). Fossil-bearing concretions of the Araripe Basin accumulated during oceanic anoxic event 1b. *Paleoceanogr. Paleoclimatol.* 38, e2023PA004736. doi:10.1029/2023PA004736

Bond, D. P. G., and Grasby, S. E. (2020). Late Ordovician mass extinction caused by volcanism, warming, and anoxia, not cooling and glaciation. *Geology* 48, 777–781. doi:10.1130/G47377.1

Bornatowski, H., Abilhoa, V., and Freitas, M. O. (2005). Alimentação da raia-viola *Zapteryx brevirostris* na Baía de Ubatuba-Enseada, São Francisco do Sul, Santa Catarina, Brasil. *Est. Biol.* 27, 31–36. doi:10.7213/reb.v27i61.22711

Brito, P. M. M. (1997). Révision des Aspidorhynchidae (Pisces, Actinopterygii) du Mésozoïque: Ostéologie, relations phylogénétiques, données environnementales et biogéographiques. *Geodiversitas* 19, 681–772.

Campbell, L., Dixon, D. G., and Hecky, R. E. (2003). A review of mercury in Lake Victoria, East Africa: implications for human and ecosystem health. *J. Toxicol. Environ. Health B* 6, 325–356. doi:10.1080/10937400306474

Cardia, F. M. S., Santucci, R. M., Bernardi, J. V. E., Andrade, M. B. de, and Oliveira, C. E. M. de (2018). Mercury concentrations in terrestrial fossil vertebrates from the Bauru Group (Upper Cretaceous), Brazil and implications for vertebrate paleontology. *J. South. Am. Earth. Sci.* 86, 15–22. doi:10.1016/j.jsames.2018.06.006

Cervini-Silva, J., Muñoz, M. de L., Palacios, E., Ufer, K., and Kaufhold, S. (2021). Natural incorporation of mercury in bone. *J. Trace Elem. Med. Biol.* 67, 126797. doi:10.1016/j.jtemb.2021.126797

Chételat, J., Amyot, M., Arp, P., Blais, J. M., Depew, D., Emmerton, C. A., et al. (2015). Mercury in freshwater ecosystems of the Canadian Arctic: recent advances on its cycling and fate. *Sci. Total Environ.* 509–510, 41–66. doi:10.1016/j.scitotenv.2014.05.151

Chiang, G., Kidd, K. A., Díaz-Jaramillo, M., Espejo, W., Bahamonde, P., O'Driscoll, N. J., et al. (2021). Methylmercury biomagnification in coastal aquatic food webs from western Patagonia and western Antarctic Peninsula. *Chemosphere* 262, 128360. doi:10.1016/j.chemosphere.2020.128360

Coutinho, D. L. C., Coutinho Júnior, J. A., Coutinho, C. C., Duque, R., Asakura, Y., Brandão, A. M., et al. (2021). A Coleção Paleontológica do Museu de Ciências Naturais e de História Barra do Jardim da Fundação Francisco de Lima Botelho, Jardim, Ceará, Brasil. *Anu. Inst. Geociênc.* 44, 35670. doi:10.11137/1982-3908_2021_44_35670

Custódio, M. A., Quaglio, F., Warren, L. V., Simões, M. G., Fürsich, F. T., Perinotto, J. A. J., et al. (2017). The transgressive-regressive cycle of the Romualdo Formation (Araripe Basin): sedimentary archive of the early cretaceous marine ingression in the interior of northeast Brazil. *Sediment. Geol.* 359, 1–15. doi:10.1016/j.sedgeo.2017.07.010

Di Beneditto, A. P. M., Bittar, V. T., Rezende, C. E., Camargo, P. B., and Kehrig, H. A. (2013). Mercury and stable isotopes (δ^{15}N and δ^{13}C) as tracers during the ontogeny of *Trichiurus lepturus*. *Neotrop. Ichthyol.* 11, 211–216. doi:10.1590/S1679-62252013000100024

Emslie, S. D., Alderman, A., McKenzie, A., Brasso, R., Taylor, A. R., Molina Moreno, M., et al. (2019). Mercury in archaeological human bone: biogenic or diagenetic? *J. Archaeol. Sci.* 108, 104969. doi:10.1016/j.jas.2019.05.005

Font, E., Adatte, T., Sial, A. N., Drude de Lacerda, L., Keller, G., and Punekar, J. (2016). Mercury anomaly, Deccan volcanism, and the end-Cretaceous mass extinction. *Geology* 44, 171–174. doi:10.1130/G37451.1

Freire, P. T. C., Silva, J. H., Sousa-Filho, F. E., Abagaro, B. T. O., Viana, B. C., Saraiva, G. D., et al. (2014). Vibrational spectroscopy and X-ray diffraction applied to the study of Cretaceous fish fossils from Araripe Basin, Northeast of Brazil. *J. Raman Spectrosc.* 45, 1225–1229. doi:10.1002/jrs.4471

Fürsich, F. T., Custódio, M. A., Matos, S. A., Hethze, M., Quaglio, F., Warren, L. V., et al. (2019). Analysis of a cretaceous (late aptian) high-stress ecosystem: the Romualdo Formation of the Araripe Basin, northeastern Brazil. *Cretac. Res.* 95, 268–296. doi:10.1016/j.cretres.2018.11.021

Gamboa Ruiz, W. L., and Tomiyasu, T. (2015). Distribution of mercury in sediments from Kagoshima Bay, Japan, and its relationship with physical and chemical factors. *Environ. Earth Sci.* 74, 1175–1188. doi:10.1007/s12665-015-4104-5

Grasby, S. E., Them, T. R., Chen, Z., Yin, R., and Ardakani, O. H. (2019). Mercury as a proxy for volcanic emissions in the geologic record. *Earth Sci. Rev.* 196, 102880. doi:10.1016/j.earscirev.2019.102880

Hamid, I., Lacerda, L. D., Saraiva, A. A. F., Sial, A. N., Benigno, A. P. A., and Aguiar, J. E. (2024). Aptian-Albian paleoenvironmental geochemistry: Araripe Basin, northeastern Brazil. *J. South. Am. Earth. Sci.* 137, 104856. doi:10.1016/j.jsames.2024.104856

Heimhofer, U., Meister, P., Bernasconi, S. M., Ariztegui, D., Martill, D. M., Rios-Netto, A. M., et al. (2017). Isotope and elemental geochemistry of black shale-hosted fossiliferous concretions from the Cretaceous Santana Formation fossil Lagerstätte (Brazil). *Sedimentology* 64, 150–167. doi:10.1111/sed.12337

Holgado, B. (2020). *New contributions to pterosaur systematics with emphasis on appendicular pneumaticity. [dissertation/PhD thesis]*. Rio de Janeiro: Federal University of Rio de Janeiro.

Hosseini, M., Nabavi, S. M. B., and Parsa, Y. (2013). Bioaccumulation of trace mercury in trophic levels of benthic, benthopelagic, pelagic fish species, and sea birds from Arvand River, Iran. *Biol. Trace Elem. Res.* 156, 175–180. doi:10.1007/s12011-013-9841-2

Kellner, A. W. A. (1996a). Fossilized theropod soft tissue. *Nat* 379, 32. doi:10.1038/379032a0

Kellner, A. W. A. (1996b). Reinterpretation of a remarkably well preserved pterosaur soft tissue from the Early Cretaceous of Brazil. *J. Vertebr. Paleontol.* 16, 718–722. doi:10.1080/02724634.1996.10011360

Kellner, A. W. A., and Campos, D. de A. (1994). A new species of *tupuxuara* (Pterosauria, tapejaridae) from the early cretaceous of Brazil. *An. Acad. Bras. Cienc.* 66, 467–474.

Kępa, M., Kozłowski, T., Szostek, K., Drozd, A., Walas, S., Mrowiec, H., et al. (2012). Analysis of mercury levels in historical bone material from syphilitic subjects - pilot studies (short report). *Anthropol. Anz.* 69, 367–377. doi:10.1127/0003-5548/2012/0163

Kim, T., Lee, Y., and Lee, Y.-N. (2018). Fluorapatite diagenetic differences between Cretaceous skeletal fossils of Mongolia and Korea. *Palaeogeogr. Palaeoclimatol. Palaeoecol.* 490, 579–589. doi:10.1016/j.palaeo.2017.11.047

Lacerda, L. D., Goyanna, F., Bezerra, M. F., and Silva, G. B. (2017). Mercury concentrations in tuna (*Thunnus albacares* and Thunnus obesus) from the Brazilian equatorial Atlantic Ocean. *Bull. Environ. Contam. Toxicol.* 98, 149–155. doi:10.1007/s00128-016-2007-0

Laurini, C. R. (2015). *Um novo olhar sobre as raias-viola (Chondrichthyes, Batoidea) do Araripe, Cretáceo Inferior do Nordeste do Brasil*. São Paulo: University of São Paulo.

Lima, F. J., Pires, E. F., Jasper, A., Uhl, D., Saraiva, A. A. F., and Sayão, J. M. (2019). Fire in the paradise: evidence of repeated palaeo-wildfires from the Araripe fossil lagerstätte (Araripe Basin, aptian-albian), northeast Brazil. *Paleobiodivers. Paleoenviron.* 99, 367–378. doi:10.1007/s12549-018-0359-7

Lima, R. C., Freire, P. de T. C., Sasaki, J. M., Saraiva, A. A. F., Lanfredi, S., and Nobre, M. A. de L. (2007). Estudo de coprólito da bacia sedimentar do Araripe por meios de espectroscopia FT-IR e difração de Raios-X. *Quim. Nova* 30, 1956–1958. doi:10.1590/S0100-40422007000800029

Lopes, G. L. B., and Barreto, A. M. F. (2021). Paleoecological and biomechanical inferences regarding the paleoichthyofauna of the Romualdo Formation, aptian-albian of the Araripe Basin, state of pernambuco, northeastern Brazil. *J. South. Am. Earth. Sci.* 111, 103444. doi:10.1016/j.jsames.2021.103444

Luo, H., Cheng, Q., and Pan, X. (2020). Photochemical behaviors of mercury (Hg) species in aquatic systems: a systematic review on reaction process, mechanism, and influencing factor. *Sci. Total Environ.* 720, 137540. doi:10.1016/j.scitotenv.2020.137540

Maisey, J. G. (1994). Predator-prey relationships and trophic level reconstruction in a fossil fish community. *Environ. Biol. Fishes* 40, 1–22. doi:10.1007/BF00002179

Maisey, J. G., and Carvalho, M. da G. P. (1995). First records of fossil sergestid decapods and fossil brachyuran crab larvae (Arthropoda, Crustacea), with remarks on some supposed palaemonid fossils, from the Santana Formation (Aptian-Albian, NE Brazil). *Am. Mus. Novit.* 20, 1–20.

Maldanis, L., Carvalho, M., Almeida, M. R., Freitas, F. I., de Andrade, J. A. F. G., Nunes, R. S., et al. (2016). Heart fossilization is possible and informs the evolution of cardiac outflow tract in vertebrates. *eLife* 5, e14698. doi:10.7554/eLife.14698

Martill, D. M. (1988). Preservation of fish in the cretaceous Santana Formation of Brazil. *Palaeontology* 31, 1–18.

Meunier, F. J., Alvarado-Ortega, J., Machado, L. P. C., and Brito, P. M. (2021). The paleohistology of bone and teeth in Cretaceous Pycnodontidae (Neopterygii: pycnodontiformes): the case of *Neoproscinetes penalvai* and *Tepexichthys aranguthyorum*. *Cybium* 45, 193–203. doi:10.26028/cybium/2021-453-003

Meyer, K. W., Petersen, S. V., Lohmann, K. C., Blum, J. D., Washburn, S. J., Johnson, M. W., et al. (2019). Biogenic carbonate mercury and marine temperature records reveal global influence of Late Cretaceous Deccan Traps. *Nat. Commun.* 10, 5356. doi:10.1038/s41467-019-13366-0

Mulder, E. W. A. (2013). On the piscivorous behaviour of the Early Cretaceous amiiform neopterygian fish *Calamopleurus cylindricus* from the Santana Formation, Northeast Brazil. *Neth. J. Geosci.* 92, 119–122. doi:10.1017/S0016774600000044

Murray, M. S., McRoy, C. P., Duffy, L. K., Hirons, A. C., Schaaf, J. M., Trocine, R. P., et al. (2015). Biogeochemical analysis of ancient Pacific Cod bone suggests Hg bioaccumulation was linked to paleo sea level rise and climate change. *Front. Environ. Sci.* 3. doi:10.3389/fenvs.2015.00008

Muto, E. Y., Soares, L. S. H., Sarkis, J. E. S., Hortellani, M. A., Petti, M. A. V., and Corbisier, T. N. (2014). Biomagnification of mercury through the food web of the Santos continental shelf, subtropical Brazil. *Mar. Ecol. Prog. Ser.* 512, 55–69. doi:10.3354/meps10892

Nursall, J. R. (1996). "Distribution and ecology of pycnodont fishes," in *Mesozoic fishes – systematics and paleoecology*. Editors A. Arratia, and G. Viohl (Munich: Verlag Dr. Friedrich Pfeil), 115–124.

Pêgas, R. V., Costa, F. R., and Kellner, A. W. A. (2021). Reconstruction of the adductor chamber and predicted bite force in pterodactyloids (Pterosauria). *Zool. J. Linn. Soc.* 193, 602–635. doi:10.1093/zoolinnean/zlaa163

Poyato-Ariza, F. J., Talbot, M. R., Fregenal-Martínez, M. A., Meléndez, N., and Wenz, S. (1998). First isotopic and multidisciplinary evidence for nonmarine coelacanths and pycnodontiform fishes: palaeoenvironmental implications. *Palaeogeogr. Palaeoclimatol. Palaeoecol.* 144, 65–84. doi:10.1016/S0031-0182(98)00085-6

Pyle, D. M., and Mather, T. A. (2003). The importance of volcanic emissions for the global atmospheric mercury cycle. *Atmos. Environ.* 37, 5115–5124. doi:10.1016/j.atmosenv.2003.07.011

Qu, P., Pang, M., Wang, P., Ma, X., Zhang, Z., Wang, Z., et al. (2022). Bioaccumulation of mercury along continuous fauna trophic levels in the Yellow River Estuary and adjacent sea indicated by nitrogen stable isotopes. *J. Hazard. Mater.* 432, 128631. doi:10.1016/j.jhazmat.2022.128631

Racki, G., Rakociński, M., Marynowski, L., and Wignall, P. B. (2018). Mercury enrichments and the Frasnian-Famennian biotic crisis: a volcanic trigger proved? *Geology* 46, 543–546. doi:10.1130/G40233.1

Rampino, M. R., Caldeira, K., and Rodriguez, S. (2024). Sixteen mass extinctions of the past 541 My correlated with 15 pulses of Large Igneous Province (LIP) volcanism and the 4 largest extraterrestrial impacts. *Glob. Planet. Change* 234, 104369. doi:10.1016/j.gloplacha.2024.104369

Ribeiro, A. C., Poyato-Ariza, F. J., Varejão, F. G., and Bockmann, F. A. (2020). The branchial skeleton in Aptian chanid fishes (Gonorynchiformes) from the Araripe Basin (Brazil): autecology and paleoecological implications. *Cretac. Res.* 112, 104454. doi:10.1016/j.cretres.2020.104454

Rosa, M. C., Morales, N., and Assine, M. L. (2023). Transtensional tectonics during the gondwana breakup in northeastern Brazil: early cretaceous paleostress inversion in the Araripe Basin. *Tectonophysics* 846, 229666. doi:10.1016/j.tecto.2022.229666

Sanei, H., Grasby, S. E., and Beauchamp, B. (2012). Latest Permian mercury anomalies. *Geology* 40, 63–66. doi:10.1130/G32596.1

Saraiva, A. A. F., Lima, F. J., Barros, O. A., and Bantim, R. A. M. (2021). *Guia de Fósseis do Araripe*. 1 ed. Crato: LPU.

Shoop, W. L., and Tilson, E. (2022). Plunge diving by brown pelicans resembles a split-S turn. *J. Field Ornithol.* 93, 2. doi:10.5751/JFO-00064-930102

Sial, A. N., Chen, J., Heriberto Peralta, S., Gaucher, C., Korte, C., Ferreira, V. P., et al. (2024). C, N, Hg isotopes and elemental chemostratigraphy across the Ordovician–Silurian transition in the Argentine Precordillera: implications for the link between volcanism and extinctions. *Gondwana Res.* 133, 270–296. doi:10.1016/j.gr.2024.06.008

Sial, A. N., Chen, J., Korte, C., Pandit, M. K., Spangenberg, J. E., Silva-Tamayo, J. C., et al. (2021). Hg isotopes and enhanced Hg concentration in the Meishan and Guryul Ravine successions: proxies for volcanism across the Permian-Triassic boundary. *Front. Earth. Sci.* 9, 651224. doi:10.3389/feart.2021.651224

Sial, A. N., Chen, J., Lacerda, L. D., Frei, R., Tewari, V. C., Pandit, M. K., et al. (2016). Mercury enrichment and Hg isotopes in Cretaceous–Paleogene boundary successions: links to volcanism and palaeoenvironmental impacts. *Cretac. Res.* 66, 60–81. doi:10.1016/j.cretres.2016.05.006

Sial, A. N., Lacerda, L. D., Ferreira, V. P., Frei, R., Marquillas, R. A., Barbosa, J. A., et al. (2013). Mercury as a proxy for volcanic activity during extreme environmental turnover: the Cretaceous–Paleogene transition. *Palaeogeogr. Palaeoclimatol. Palaeoecol.* 387, 153–164. doi:10.1016/j.palaeo.2013.07.019

Silva Santos, R. D. (1995). *Santanichthys*, novo epíteto genérico para *Leptolepis diasii* Silva Santos, 1958 (Pisces, Teleostei) da Formação Santana (Aptiano), Bacia do Araripe, NE do Brasil. *An. Acad. Brasil. Ci.* 67, 249–258.

Sousa Filho, F. E., Silva, J. H. da, Saraiva, G. D., Abagaro, B. T. O., Barros, O. A., Saraiva, A. A. F., et al. (2016). Spectroscopic studies of the fish fossils (*Cladocyclus gardneri* and *Vinctifer comptoni*) from the ipubi Formation of the cretaceous period. *Spectrochim. Acta A Mol. Biomol. Spectrosc.* 157, 124–128. doi:10.1016/j.saa.2015.12.022

Starr, L. D., McCarthy, M. J., Hammerschmidt, C. R., Subramaniam, A., Despins, M. C., Montoya, J. P., et al. (2022). Mercury methylation linked to nitrification in the tropical North Atlantic Ocean. *Mar. Chem.* 247, 104174. doi:10.1016/j.marchem.2022.104174

Sun, R., Jiskra, M., Amos, H. M., Zhang, Y., Sunderland, E. M., and Sonke, J. E. (2019). Modelling the mercury stable isotope distribution of Earth surface reservoirs: implications for global Hg cycling. *Geochim. Cosmochim. Acta* 246, 156–173. doi:10.1016/j.gca.2018.11.036

Thibodeau, A. M., Ritterbush, K., Yager, J. A., West, A. J., Ibarra, Y., Bottjer, D. J., et al. (2016). Mercury anomalies and the timing of biotic recovery following the end-Triassic mass extinction. *Nat. Commun.* 7, 11147. doi:10.1038/ncomms11147

Trevizani, T. H., Figueira, R. C. L., Santos, M. C. de O., and Domit, C. (2021). Mercury in trophic webs of estuaries in the southwest Atlantic Ocean. *Mar. Pollut. Bull.* 167, 112370. doi:10.1016/j.marpolbul.2021.112370

Wang, J., Dai, J., Chen, G., and Jiang, F. (2022). Role of sulfur biogeochemical cycle in mercury methylation in estuarine sediments: a review. *J. Hazard. Mater.* 423, 126964. doi:10.1016/j.jhazmat.2021.126964

Wang, Y., Roth, S., Schaefer, J. K., Reinfelder, J. R., and Yee, N. (2020). Production of methylmercury by methanogens in mercury contaminated estuarine sediments. *FEMS Microbiol. Lett.* 367, fnaa196. doi:10.1093/femsle/fnaa196

Wilby, P. R., and Martill, D. M. (1992). Fossil fish stomachs: a microenvironment for exceptional preservation. *Hist. Biol.* 6, 25–36. doi:10.1080/10292389209380416

Witton, M. P. (2013). *Pterosaurs: natural history, evolution, anatomy*. Princeton: Princeton University Press.

Zhou, Y., Li, Y., Zheng, W., Tang, S., Pan, S., Chen, J., et al. (2024). The role of LIPs in Phanerozoic mass extinctions: an Hg perspective. *Earth Sci. Rev.* 249, 104667. doi:10.1016/j.earscirev.2023.104667